



HAL
open science

The intraflagellar transport dynein complex of trypanosomes is made of a heterodimer of dynein heavy chains and of light and intermediate chains of distinct functions

Thierry Blisnick, Johanna Buisson, Sabrina Absalon, Alexandra Marie, Nadège Cayet, Philippe Bastin

► To cite this version:

Thierry Blisnick, Johanna Buisson, Sabrina Absalon, Alexandra Marie, Nadège Cayet, et al.. The intraflagellar transport dynein complex of trypanosomes is made of a heterodimer of dynein heavy chains and of light and intermediate chains of distinct functions. *Molecular Biology of the Cell*, 2014, 25 (17), pp.2620-2633. 10.1091/mbc.E14-05-0961 . pasteur-01301215

HAL Id: pasteur-01301215

<https://pasteur.hal.science/pasteur-01301215>

Submitted on 11 Apr 2016

HAL is a multi-disciplinary open access archive for the deposit and dissemination of scientific research documents, whether they are published or not. The documents may come from teaching and research institutions in France or abroad, or from public or private research centers.

L'archive ouverte pluridisciplinaire **HAL**, est destinée au dépôt et à la diffusion de documents scientifiques de niveau recherche, publiés ou non, émanant des établissements d'enseignement et de recherche français ou étrangers, des laboratoires publics ou privés.



Distributed under a Creative Commons Attribution - NonCommercial 4.0 International License

The intraflagellar transport dynein complex of trypanosomes is made of a heterodimer of dynein heavy chains and of light and intermediate chains of distinct functions

Thierry Blisnick^a, Johanna Buisson^a, Sabrina Absalon^a, Alexandra Marie^a, Nadège Cayet^b, and Philippe Bastin^a

^aTrypanosome Cell Biology Unit, Institut Pasteur, and Centre National de la Recherche Scientifique URA 2581, 75015 Paris, France; ^bImagopole Platform, Institut Pasteur, 75015 Paris, France

ABSTRACT Cilia and flagella are assembled by intraflagellar transport (IFT) of protein complexes that bring tubulin and other precursors to the incorporation site at their distal tip. Anterograde transport is driven by kinesin, whereas retrograde transport is ensured by a specific dynein. In the protist *Trypanosoma brucei*, two distinct genes encode fairly different dynein heavy chains (DHCs; ~40% identity) termed DHC2.1 and DHC2.2, which form a heterodimer and are both essential for retrograde IFT. The stability of each heavy chain relies on the presence of a dynein light intermediate chain (DLI1; also known as XB1/D1bLIC). The presence of both heavy chains and of DLI1 at the base of the flagellum depends on the intermediate dynein chain DIC5 (FAP133/WDR34). In the *IFT140^{RNAi}* mutant, an IFT-A protein essential for retrograde transport, the IFT dynein components are found at high concentration at the flagellar base but fail to penetrate the flagellar compartment. We propose a model by which the IFT dynein particle is assembled in the cytoplasm, reaches the base of the flagellum, and associates with the IFT machinery in a manner dependent on the IFT-A complex.

Monitoring Editor
Keith G. Kozminski
University of Virginia

Received: May 7, 2014
Revised: Jun 19, 2014
Accepted: Jun 20, 2014

INTRODUCTION

Intraflagellar transport (IFT) is the movement of two protein complexes termed IFT-A and IFT-B from the base of cilia and flagella to their tip (anterograde) and back (retrograde transport; Kozminski et al., 1993; Rosenbaum and Witman, 2002). IFT takes place along microtubules and is driven by motors belonging to the kinesin and

the dynein family. IFT likely transports flagellar precursors for their incorporation at the distal tip of the elongating flagellum (Wren et al., 2013) and accordingly is required for construction in most species examined to date. Much attention has been devoted to the IFT-B complex (Bhogaraju et al., 2013b) and to the kinesin motors (Scholey, 2013), whereas data on IFT-A and dynein motors are comparatively scarce. However, the recent discovery that several ciliopathies (genetic diseases due to malfunctioning of cilia and flagella) are caused by mutations in genes encoding IFT-A or dynein components has led to interest in further investigation (Dagoneau et al., 2009; Gilissen et al., 2010; Walczak-Sztulpa et al., 2010; Arts et al., 2011; Bredrup et al., 2011; Davis et al., 2011; Perrault et al., 2012; Huber et al., 2013; Schmidts et al., 2013). Inhibition of retrograde IFT results in the formation of shorter cilia and flagella, which accumulate IFT material mostly belonging to the IFT-B complex (Pazour et al., 1999; Porter et al., 1999; Blacque et al., 2006; Absalon et al., 2008b). Biochemical studies in *Chlamydomonas* revealed that the IFT dynein responsible for retrograde IFT is made of a homodimer of a specific dynein heavy chain (DHC2, also known as DHC1b) associated with a dynein light intermediate chain (LIC) (DLI1, also known as

This article was published online ahead of print in MBoC in Press (<http://www.molbiolcell.org/cgi/doi/10.1091/mbc.E14-05-0961>) on July 2, 2014.

T.B. designed and performed the majority of the experiments, analyzed the data, and generated the figures. J.B., S.A., A.M., and N.C. performed some of the reported experiments and analyses. P.B. supervised the project, assisted with experimental design and analyses, and wrote the manuscript.

The authors declare that there is no conflict of interest.

Address correspondence to: Philippe Bastin (pbastin@pasteur.fr).

Abbreviations used: DHC, dynein heavy chain; DIC, dynein IC; DLI, dynein light IC; EGFP, enhanced green fluorescent protein; IFA, immunofluorescence assay; IFT, intraflagellar transport; RNAi, RNA interference.

© 2014 Blisnick et al. This article is distributed by The American Society for Cell Biology under license from the author(s). Two months after publication it is available to the public under an Attribution–Noncommercial–Share Alike 3.0 Unported Creative Commons License (<http://creativecommons.org/licenses/by-nc-sa/3.0>).

“ASCB®,” “The American Society for Cell Biology®,” and “Molecular Biology of the Cell®” are registered trademarks of The American Society of Cell Biology.

Supplemental Material can be found at:
<http://www.molbiolcell.org/content/suppl/2014/06/30/mbc.E14-05-0961v1.DC1.html>

D1bLIC or XB1), a dynein IC (DIC5, also known as FAP133/WDR34), and a light chain (LC8; Rompolas *et al.*, 2007). More recently, an additional IC termed FAP163/WD60 was identified and associates with DIC5 (Patel-King *et al.*, 2013). Most of these proteins turned out to be required for proper retrograde transport (Pazour *et al.*, 1998, 1999; Porter *et al.*, 1999; Schafer *et al.*, 2003; Patel-King *et al.*, 2013), although the individual contribution of each remains to be clarified.

The protist *Trypanosoma brucei* is emerging as a potent model to study the flagellum (Baron *et al.*, 2007), especially its formation, bringing complementary information to the well-established *Chlamydomonas* model (Morga and Bastin, 2013). The cell possesses a long flagellum (~22 μm in the culture-adapted procyclic stage), and IFT can be monitored and quantified using fusion proteins (Absalon *et al.*, 2008b). Curiously, two clearly distinct genes for the IFT dynein heavy chain are predicted in the genome, a feature conserved in all members of the Trypanosomatid family (Adhiambo *et al.*, 2005). These are termed DHC2.1 and DHC2.2. In the related protist *Leishmania mexicana* (in which flagella do not appear to be essential, at least in culture), only DHC2.2 could be deleted by gene knockout, which resulted in the formation of tiny flagella. In contrast, DHC2.1-knockout cells could not be obtained, leading to the suggestions that the gene was essential and that the two heavy chains perform separate functions (Adhiambo *et al.*, 2005). In *T. brucei*, DHC2.1 exhibited both anterograde and retrograde IFT upon endogenous tagging with green fluorescent protein (GFP), suggesting that it participates in IFT (Buisson *et al.*, 2013). Knockdown of the other dynein heavy chain, DHC2.2, by RNA interference (RNAi) inhibited flagellum formation (Kohl *et al.*, 2003), and preliminary electron microscopy analysis indicated the presence of short flagella containing electron-dense material, which could well be typical of retrograde transport defects (Absalon *et al.*, 2008b).

In this study, the role of four distinct components of the trypanosome IFT dynein is investigated in detail. Surprisingly, the two heavy chains, DHC2.1 and DHC2.2, are not redundant and both turn out to be essential for retrograde transport. Immunoprecipitation data indicate that they form a heterodimer, a unique fact for IFT dyneins. An essential contribution to retrograde IFT is shown for DLI1 as in green algae and nematodes, and for the first time for DIC5. Further analysis reveals that DLI1 is required for the stability of the dynein heavy chains and that DIC5 contributes to localization of the dynein components from the cytoplasm to the base of the flagellum. Finally, the relationship with the IFT-A complex, the other key player in retrograde transport, is examined, revealing a critical role for the entry of the dynein complex in the flagellar compartment but not for its assembly. These data lead to a new molecular model explaining the formation and functioning of the IFT dynein complex.

RESULTS

The IFT dynein is composed of different subunits

Genome analysis revealed the presence of two clearly distinct genes coding for the IFT dynein heavy chain, which were termed *DHC2.1* (Tb927.4.560) and *DHC2.2* (Tb927.11.2430; Briggs *et al.*, 2004; Adhiambo *et al.*, 2005; Berriman *et al.*, 2005; Kohl and Bastin, 2005; Figure 1A). This duplication appears specific to kinetoplastids, as both genes are found in the genomes of African trypanosomes (*T. brucei*, *T. brucei gambiense*, *T. congolense*, and *T. vivax*), of the more distant South American trypanosome *T. cruzi*, and of all *Leishmania* subspecies (*L. mexicana*, *L. major*, *L. braziliensis*, and *L. infantum*). When compared with the corresponding IFT dynein heavy chain from humans, *Caenorhabditis reinhardtii*, or *Caenorhabditis elegans*, DHC2.1 and DHC2.2 share 33–39% identity and

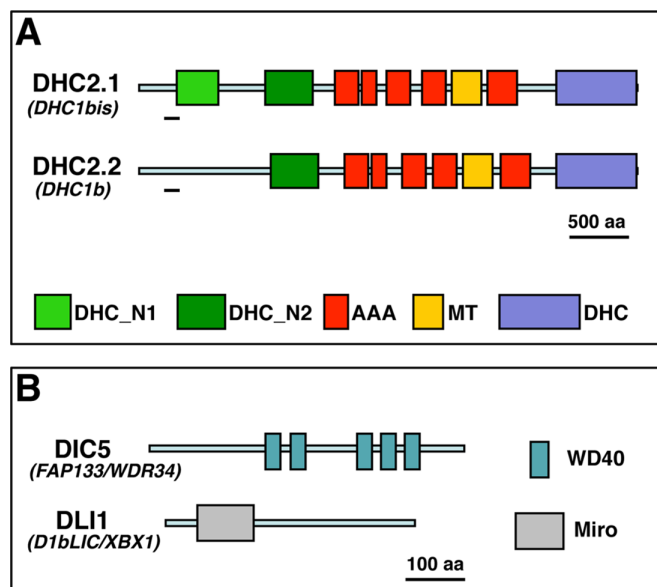


FIGURE 1: Proteins comprising the IFT dynein complex in *T. brucei* investigated in this study. (A) The two heavy chains, DHC2.1 and DHC2.2. (B) The two associated chains, DLI1 and DIC5. The existence of specific domains (shown as large boxes) was determined by Pfam analysis (Finn *et al.*, 2014). DHC2.1 possesses two typical N-terminal domains of dynein heavy chains (green), whereas only one is present in DHC2.2. AAA, domains associated with ATPase activity (red); DHC, signature for dynein heavy chains (blue); Miro, domain originally found in mitochondrial Rho GTPases with tandem GTP binding and two EF-hand domains; MT, microtubule-binding domain (yellow); WD40, domain rich in tryptophan and aspartate (dark blue). The black lines indicate the portions selected to express polypeptides used for antibody production. These portions are extremely divergent and share <15% identity.

54–59% similarity. Much greater conservation is found in the typical dynein signatures (Supplemental Figure S1). DHC2.1 and DHC2.2 possess the three-amino acid insertion A-G-K found between the first two P-loops that is typical of IFT dynein heavy chains (Pazour *et al.*, 1999). This signature is conserved in predicted DHC2 proteins from 30 different species ranging from protists to mammals (unpublished data). Alignment of the *T. brucei* DHC2.1 and DHC2.2 reveals that they share only 39% identity, a feature conserved among the other trypanosomatids. Nevertheless, all typical domains of dynein heavy chains are present, such as AAA (ATPase associated), the microtubule-binding domain, and the C-terminal signature (Figure 1A). The main difference between these two heavy chains is the absence of the dynein N-terminal region 1 from the DHC2.2 from all five species examined (Figure 1A). This region has been proposed to mediate interaction with light and intermediate chains (Sakato and King, 2004). Therefore trypanosomatids harbor two clearly distinct genes potentially encoding IFT dynein heavy chains. A dynein light IC (DLI1) and a dynein IC (DIC5) were also identified (Figure 1B) and will be discussed.

DHC2.1 and DHC2.2 are essential for retrograde transport

DHC2.1 and DHC2.2 are found in the intact flagellum proteome of procyclic *T. brucei*, suggesting that they could be flagellar proteins (Subota *et al.*, 2014). To evaluate their exact localization, we produced polyclonal antibodies against the highly divergent N-terminal regions using amino acids (aa) 326–488 of DHC2.1 and 308–509 of DHC2.2 (Figure 1A). By immunofluorescence assay (IFA) on

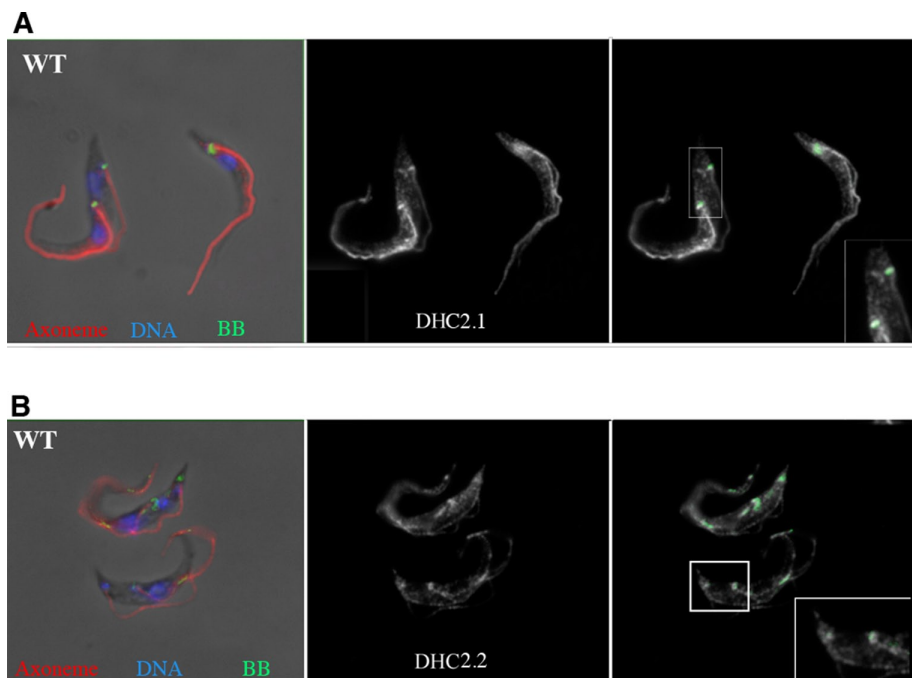


FIGURE 2: Both dynein heavy chains display typical location of IFT proteins. Wild-type cells (WT) were stained with the axoneme marker Mab25 (red), the basal body marker Mab22 (green), and DAPI (blue; left). The distribution of DHC2.1 (A) and DHC2.2 (B) is shown in white either alone (middle) or with the basal body marker (green, right). Both dyneins are found in the flagellum, at the flagellar base, and in the cytoplasm.

methanol-fixed trypanosomes, both antibodies produced staining all along the length of the flagellum and regularly lit up the base of the flagellum (Figure 2, A and B). The later signal was found above the Mab22 signal, a marker of the basal body (Bonhivers *et al.*, 2008). Some signal was also detected in the cytoplasm. This staining pattern is similar to what was observed for several trypanosome IFT-B proteins (Absalon *et al.*, 2008b; Adhiambo *et al.*, 2009; Franklin and Ullu, 2010; Bhogaraju *et al.*, 2013a; Huet *et al.*, 2014).

To confirm protein distribution and to evaluate their ability to participate to IFT, we expressed N-terminal enhanced GFP (EGFP) fusion proteins upon endogenous tagging. Western blot validated

the expression of both EGFP::DHC2.1 and EGFP::DHC2.2 displaying the expected motility on gel (Figure 3A). Analysis of live cells demonstrated that both EGFP::DHC2.1 (Buisson *et al.*, 2013) and EGFP::DHC2.2 (Figure 3B) were concentrated at the flagellar base and moving rapidly in both anterograde and retrograde directions in the flagellum (Supplemental Video S1). Kymograph analysis revealed robust anterograde and retrograde IFT (Figure 3C). Anterograde trains looked longer, traveled more slowly, and were less frequent than retrograde trains, in agreement with what was reported previously for two IFT-B components (GFP::IFT52 and YFP::IFT81) or for the dynein heavy chain GFP::DHC2.1 (Bhogaraju *et al.*, 2013a; Buisson *et al.*, 2013). These data demonstrate that both DHC2.1 and DHC2.2 are well related to IFT.

To determine the contributions of these two very distinct dynein heavy chains to IFT, we knock down their expression by RNAi upon transfection of a vector allowing inducible expression of double-stranded RNA of *DHC2.1* or *DHC2.2* (Figure 4). In both cases, Western blot confirmed potent silencing (Figure 4A), and IFA revealed a severe drop in the amount of detected protein, including at the base of flagellum (Supplemental

Figure S2 for DHC2.1 and Supplemental Figure S3 for DHC2.2). Observation of live trypanosomes of induced *DHC2.1^{RNAi}* and of the *DHC2.2^{RNAi}* strains showed that cells assembled shorter flagella, whereas flagella assembled before RNAi remained in place, as reported for other *IFT^{RNAi}* mutants (Kohl *et al.*, 2003). To understand the nature of the defect in flagellum assembly, we induced the *DHC2.1^{RNAi}* and *DHC2.2^{RNAi}* strains for 3 d and analyzed them by IFA and electron microscopy. First, IFA using the anti-IFT172 marker antibody revealed that formation of shorter flagella was accompanied by a spectacular accumulation of IFT protein in both cases (Figure 4B). Second, scanning electron microscopy showed the presence

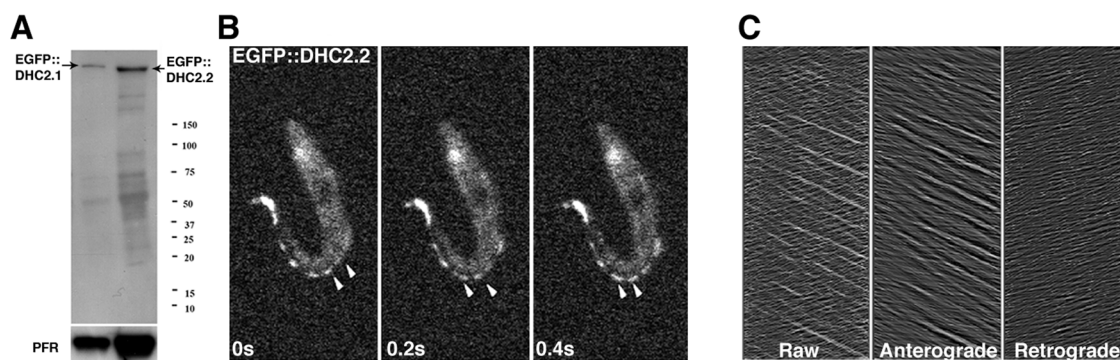


FIGURE 3: Dynein heavy chains display classic IFT when fused to EGFP. (A) Western blot of total protein extracts from cell lines expressing EGFP::DHC2.1 or EGFP::DHC2.2 probed with an anti-GFP antibody. The positions of molecular weight markers are indicated. The expected position of each fusion protein is marked with an arrow. (B) Still images from Supplemental Video S1 showing the movement of several trains containing EGFP::DHC2.2. The timing is indicated, and the arrowheads point to two trains showing anterograde movement. (C) A kymograph was extracted from Supplemental Video S1 showing robust anterograde and retrograde transport that could be separated as previously described (Chenouard *et al.*, 2010; Buisson *et al.*, 2013).

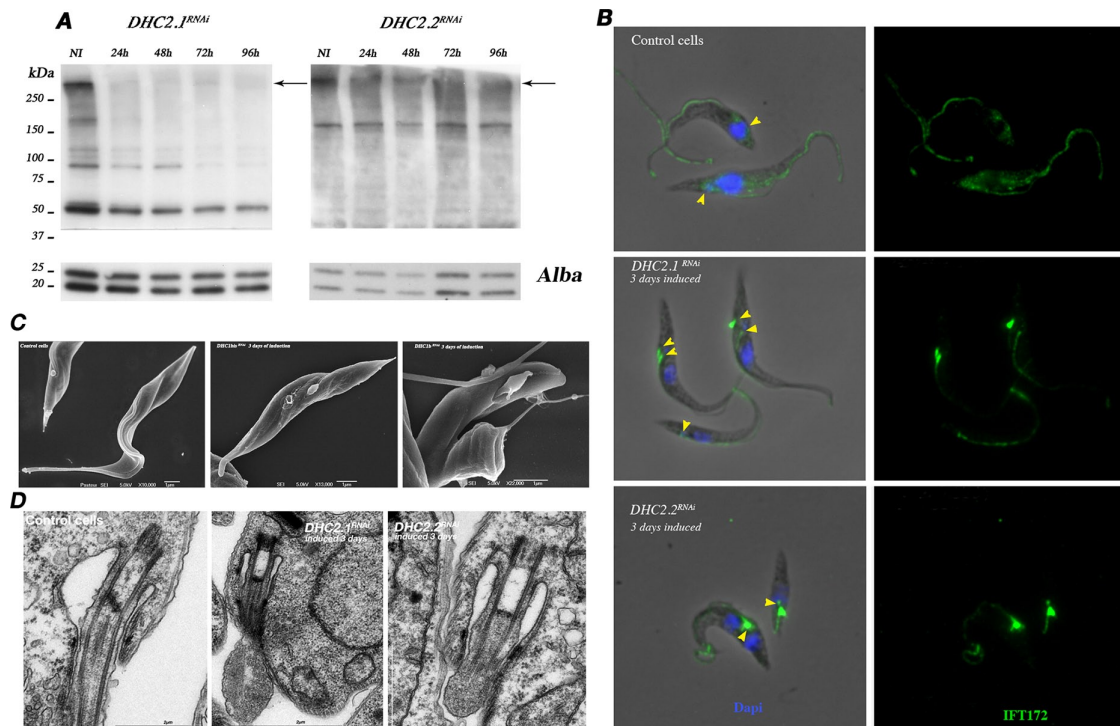


FIGURE 4: DHC2.1 and DHC2.2 are not redundant and are both essential for retrograde IFT. (A) Western blot showing depletion of DHC2.1 and DHC2.2 upon RNAi silencing in the *DHC2.1^{RNAi}* and *DHC2.2^{RNAi}* cell lines. Cells were grown in the presence of tetracycline for the indicated periods of time. Total protein samples were separated by SDS-PAGE, blotted onto a PVDF membrane, and incubated with the indicated antibodies. The anti-ALBA antibody was used as a loading control. The arrows indicate the positions of DHC2.1 and DHC2.2, respectively. (B) IFA using the anti-IFT172 antibody (green) counterstained with DAPI (blue) in the indicated cell lines and conditions. The protein shows massive accumulation in the short flagella of the induced populations. Yellow arrows indicate the base of the flagellum. (C) Scanning electron microscopy analysis revealed the presence of a long flagellum and the typical elongated trypanosome shape in noninduced controls (left), whereas only a short, dilated flagellum is visible on induced *DHC2.1^{RNAi}* (middle) and *DHC2.2^{RNAi}* (right) cells, which exhibit the modified shape typical of IFT mutants. (D) Section through the flagellar base in control cells (left) showing the typical organization with the basal body, the transition zone, and the axoneme emerging from the flagellar pocket. In contrast, in both induced *DHC2.1^{RNAi}* (middle) and *DHC2.2^{RNAi}* (right) cells, the axoneme barely reaches the tip of the flagellar pocket, and significant amounts of electron-dense material accumulate, even dilating the flagellum membrane.

of short and dilated flagella barely emerging from the flagellar pocket (Figure 4C). Analysis of successive induction times revealed that the length of the flagellum was becoming shorter and shorter for both cell lines (Supplemental Figure S4). Third, transmission electron microscopy revealed that the dilation corresponded to an accumulation of electron-dense material (Figure 4D). The presence of a short and ill-organized axoneme was also observed with microtubules ending prematurely. These results are typical of inhibition of retrograde transport, leading to the conclusion that both DHC2.1 and DHC2.2 are essential for retrograde transport.

DHC2.1 and DHC2.2 form a heterodimer

Cytoplasmic or IFT dyneins were only known to function as homodimers of heavy chains associated with various light and intermediate chains (Vale, 2003; Rompolas *et al.*, 2007), raising a question about the unexpected nonredundant roles of DHC2.1 and DHC2.2 in trypanosomes. Two possibilities can be considered: the existence of two separate homodimers or the presence of a single heterodimer. Western blot was used to evaluate the consequence of the loss of one heavy chain for the abundance of the other one. Surprisingly, knockdown of DHC2.2 resulted in severe reduction in the amount of DHC2.1 protein (Figure 5A). This suggests that DHC2.1 relies on

DHC2.2 for stability, and therefore we considered the possibility that they could associate to form a heterodimer. To this end, we carried out several immunoprecipitation assays with a combination of antibodies and cell lines. First, lysates of the GFP::DHC2.1 cell line were incubated with an anti-GFP to immunoprecipitate the fusion protein. Precipitates were probed by immunoblot with the anti-DHC2.2 antibody, revealing the presence of EGFP::DHC2.1 (Figure 5B, lane 1). When the same experiment was performed with wild-type samples, no signal was detected (Figure 5B, lane 2). This result implies an association of DHC2.1 with EGFP::DHC2.2 and supports the existence of a heterodimer of heavy chains. Next the anti-DHC2.1 was used to immunoprecipitate the protein from wild-type cell lysates, and the pellet was probed with the anti-DHC2.2, also revealing a positive interaction (Figure 5B, lane 3). In another series of experiment, lysates of the EGFP::DHC2.1 cell line were incubated with the anti-DHC2.2, and immunoblotting with an anti-DHC2.2 antibody detected a positive signal (Figure 5B, lane 4). In contrast, a negative control using the anti-GFP in the precipitation step did not produce a positive signal when probing with the anti-DHC2.1 antibody. These results support the existence of a heterodimer of DHC2.1 and DHC2.2 and explain the nonredundancy of both dynein heavy chains in retrograde transport.

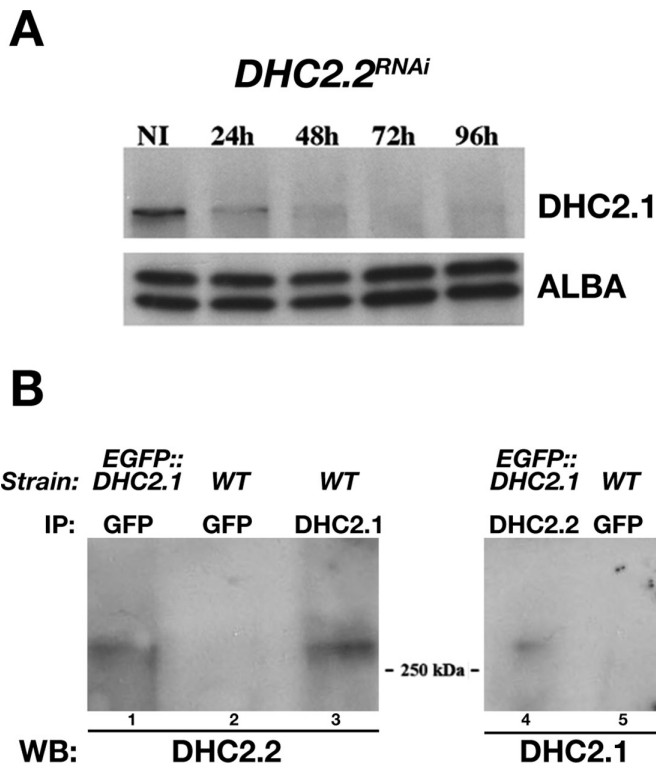


FIGURE 5: DHC2.1 and DHC2.2 form a heterodimer. (A) Western blot of total protein samples of *DHC2.2^{RNAi}* cells grown in the absence or in presence of tetracycline for the indicated periods and probed with the anti-DHC2.1 antibody. (B) Immunoprecipitation assays revealing interactions between DHC2.1 and DHC2.2. Lysates from the indicated cell lines were incubated with the antibody shown on the top and with protein A beads. Precipitates were run on SDS-PAGE, transferred to membranes, and probed with the antibodies indicated at the bottom.

Two nonmotor IFT dynein subunits are also essential for retrograde transport

The dynein heavy chains function within a protein complex associated with various intermediate and light chains. Here we followed the recently unified nomenclature for naming them (Hom *et al.*, 2011). Although trypanosomes possess two genes encoding IFT dynein heavy chains, only a single gene could be found for the dynein IC 5 (DIC5), also known as FAP133 (Rompolas *et al.*, 2007), and for the dynein light IC 1 (DLI1), also known as XBX1 (Schafer *et al.*, 2003) or D1bLIC (Hou *et al.*, 2004; Figure 1B). DIC5 exhibits 5 WD40 repeats according to Pfam analysis and shares 31% identity and 48% similarity with orthologues in human or in *Chlamydomonas*. The *T. brucei* DIC5 sequence (Tb927.3.5540) has distant but significant similarity with four other dynein intermediate chains that also contain WD40 repeats: IC78 or DNAI1, IC70 or DNAI2—both components of the axonemal outer dynein arm—and IC138 and IC140, which are associated with some axonemal inner dynein arms. In the case of DLI1, the *T. brucei* protein (encoded by Tb927.11.16810) shares 26–27% identity and 43–47% similarity with the corresponding protein from humans, worms, or algae. The Miro-1 domain found at the N-terminal part is conserved in all trypanosomatids (Figure 1B). Miro stands for mitochondrial Rho proteins, atypical Rho GTPases that have a unique domain organization, with tandem GTP-binding domains and two EF hand domains that may bind calcium. No other related proteins could be found in any of the trypanosome genomes.

To evaluate the role and the possible contribution of these two proteins to retrograde transport in *T. brucei*, they were first fused to GFP upon endogenous tagging. Western blot using the anti-GFP antibody confirmed the presence of the fusion proteins displaying the expected motility corresponding to 73 kDa for EGFP::DLI1 and 86 kDa for EGFP::DIC5 (Figure 6A). IFA with the anti-GFP and observation of live cells revealed a similar location as previously shown for the dynein heavy chains: concentration at the flagellar base, distribution all along the flagellum, and a diffuse cytoplasmic presence (Figure 6B). Analysis of live cells demonstrated robust anterograde IFT for both fusion proteins (Supplemental Videos S2 and S3 and still images in Figure 6C). However, the fluorescence signal was somehow weaker compared with GFP fused to dynein heavy chains, and the smaller retrograde trains were more discrete, especially because of their masking by the longer anterograde trains. To confirm the existence of retrograde transport, we extracted anterograde and retrograde trafficking independently from kymographs (Chenouard *et al.*, 2010). Such an analysis revealed the frequent presence of fast retrograde trains in addition to the slower and larger anterograde trains (Supplemental Figure S5).

RNAi targeting of DLI1 or of DIC5 produced a typical phenotype related to inhibition of retrograde transport: cells assembled short, dilated flagella, as visualized by scanning electron microscopy (Figure 7A), and these were filled with IFT material, as shown by IFA with the anti-IFT172 antibody (Figure 7B). To quantify the penetrance of the phenotype, we analyzed induced *DLI1^{RNAi}* and *DIC5^{RNAi}* cells by IFA using the anti-IFT172 and the anti-axoneme marker Mab25 and compared them with the typical retrograde mutants *DHC2.1^{RNAi}* and *IFT140^{RNAi}* (Supplemental Figure S6). The following typical cell types were scored: 1) with a normal-looking flagellum; 2) with a flagellum that is too short (<10 μ m), typical of early stages of knockdown (Kohl *et al.*, 2003); 3) with a normal-looking old flagellum and an abnormally short new flagellum filled with IFT material (typical of the emergence of the retrograde phenotype); 4) with a short flagellum (<5 μ m) filled with IFT material (the archetype of the retrograde phenotype); and 5) with a short flagellum (<5 μ m) but without excessive IFT amount (seen at later time points). The kinetics of emergence of the different populations was quite similar in all cases and comparable to that of previously reported retrograde transport mutants (Absalon *et al.*, 2008a). This demonstrates that although they are deprived of ATPase activity, these two dynein subunits are essential for retrograde IFT.

DLI1 and DIC5 perform separate functions

To find out the exact role of these dynein subunits, the behavior of the dynein heavy chain was examined closely in each mutant. First, Western blot using the anti-DHC2.1 antibody revealed a severe reduction in the amount of this heavy chain in the *DLI1^{RNAi}* mutant (Figure 8A), whereas only a modest reduction was noted in the *DIC5^{RNAi}* mutant (Figure 9A). This was confirmed upon expression of the GFP::DHC2.1 fusion protein in the *DLI1^{RNAi}* mutant. Whereas noninduced cells showed the typical presence of the fluorescent dynein heavy chain protein in the flagellum and at its base, the signal dropped quickly during the course of induction and was barely detectable after 3 d of growth in RNAi conditions (Figure 8B). In contrast, the same GFP::DHC2.1 reporter protein was still detected in the *DIC5^{RNAi}* mutant, but the signal was very diffuse throughout the cell, with far less protein being found in the flagellum or at the flagellar base (Figure 9B). The dynein heavy chain was not found in the short flagella. These results suggest that DLI1 is essential for heavy chain stability and that DIC5 is important for targeting the heavy chain to the base of the flagellum.

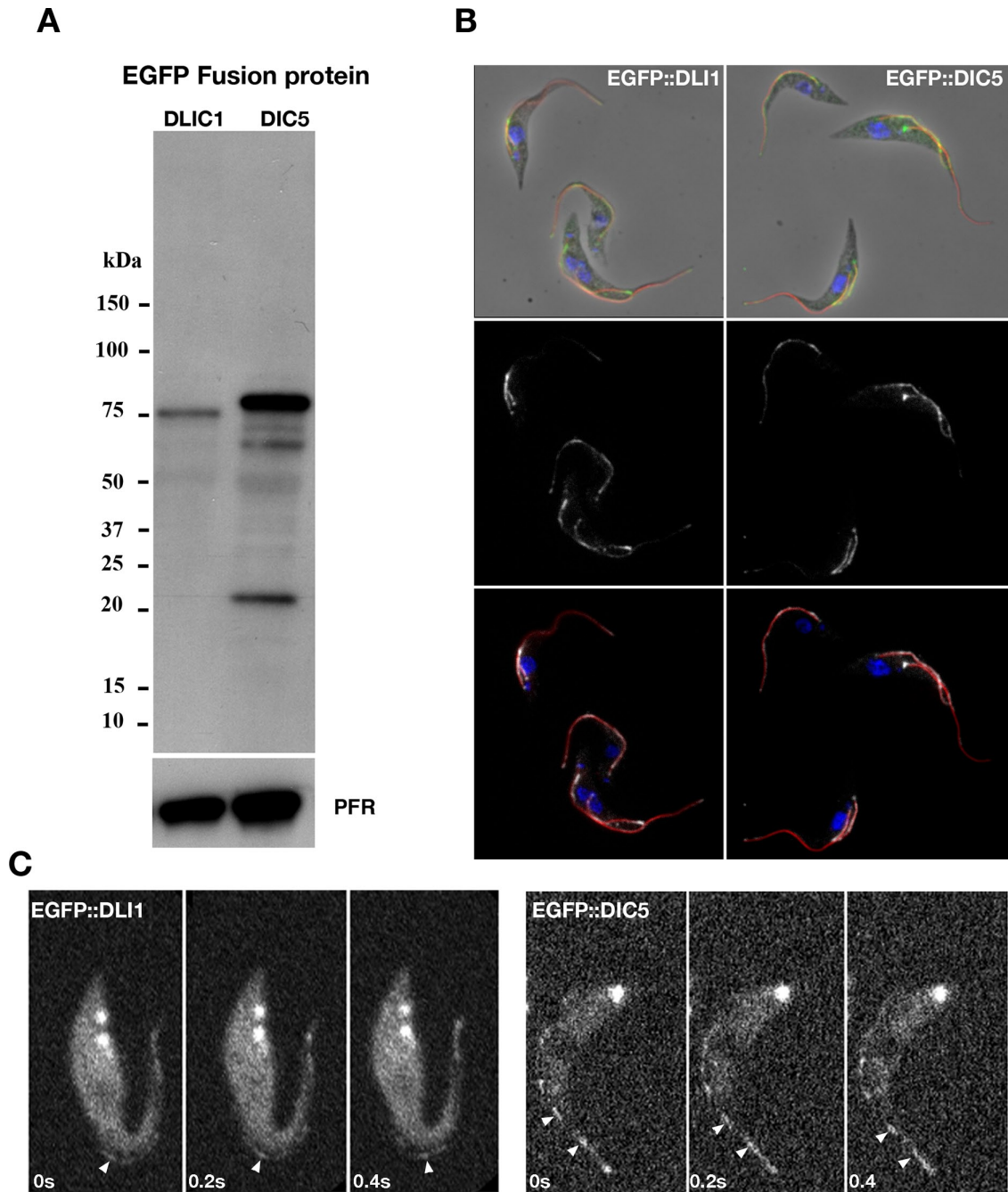


FIGURE 6: DLI1 and DIC5 are flagellar proteins that display IFT. (A) Western blot of total protein extracts from cell lines expressing EGFP::DLI1 or EGFP::DIC5 and probed with an anti-GFP antibody. The L13D6 antibody detecting the paraflagellar rod (PFR) proteins was used as a loading control. (B) Cells expressing EGFP::DLI1 (left) or EGFP::DIC5 (right) were stained with the axoneme marker Mab25 (red) and the anti-GFP (green on top row, white in other lanes). Slides were counterstained with DAPI (blue) to reveal DNA in the nucleus and the kinetoplast. Both dynein chains are found in the flagellum, at the flagellar base, and in the cytoplasm. (C) Still images of cells expressing EGFP::DLI1 or EGFP::DIC5 at the indicated time point at two trains showing anterograde movement.

To determine whether these conclusions could apply to other components of the IFT dynein complex, we transfected each RNAi mutant with the construction expressing either GFP::DLI1 or GFP::DIC5 (Table 1), in order to monitor the fate of the other light or IC. In the *DLI1^{RNAi}* cell line, a significant reduction in the amount of detectable DIC5 protein was observed, but its localization at the flagellar base seemed conserved (Figure 8C). In the other situation, the amount of DLI1 was not visibly affected in the *DIC5^{RNAi}* cell line,

but its distribution became cytoplasmic without precise location to the flagellar base or to the flagellum (Figure 9C). In both cases, the dynein subunits were not found in the short flagella, whose presence was confirmed by the Mab25 axoneme marker (Figures 8C and 9C). We conclude that DLI1 plays a central role in the stability or formation of the IFT dynein complex. DIC5 is not necessary for the stability of the dynein heavy chains, but instead is involved in their targeting to the base of the flagellum, since a dispersion of heavy

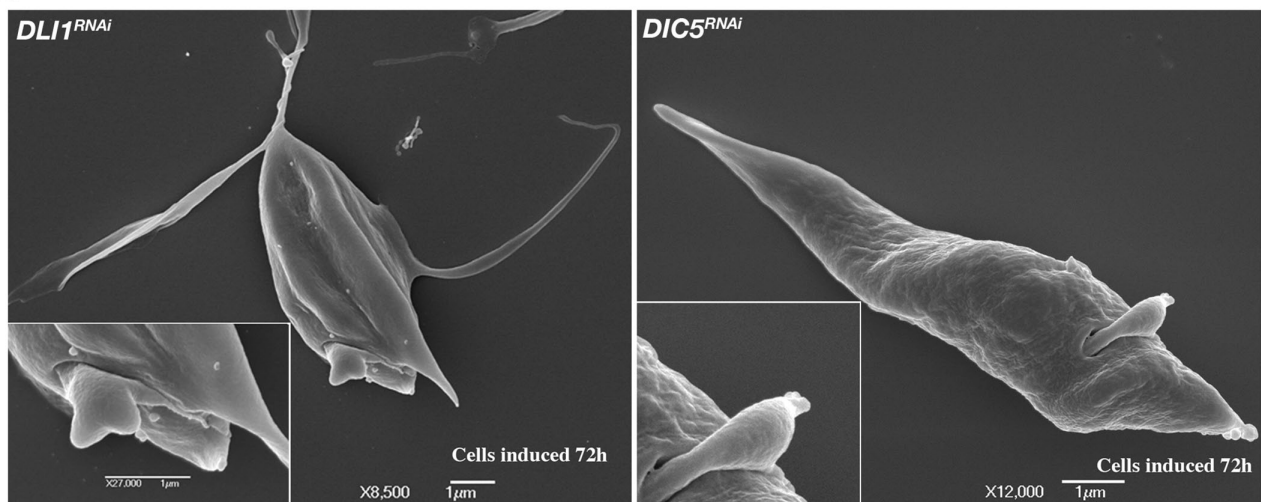
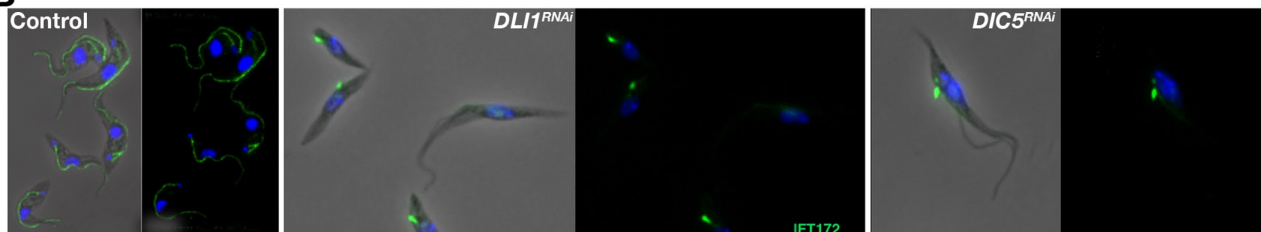
A**B**

FIGURE 7: DLI1 and DIC5 are essential for retrograde transport. (A) Scanning electron microscopy analysis of induced *DLI1*^{RNAi} (left) or *DIC5*^{RNAi} (right) cells showing the presence of short, dilated flagella barely emerging from the flagellar pocket and the typical cellular shape observed in the absence of a normal-length flagellum. The long protrusion seen on the right of the *DLI1*^{RNAi}-induced cell is not related to flagella but is a classic consequence of poor cytokinesis, a frequent feature in mutants deprived of normal flagella (Absalon *et al.*, 2008b). (B) IFA using the anti-IFT172 antibody (green) counterstained with DAPI (blue) in the indicated cell lines and conditions. The protein shows massive accumulation in the short flagella.

and light intermediate chains throughout the cytoplasm is observed in the *DIC5*^{RNAi} cell line.

The complex A IFT140 protein is required for entry of the IFT dynein components in the flagellum

In addition to the IFT dynein, the IFT-A complex is also essential to retrograde transport, although its exact function in this process remains elusive. The behavior of different subunits of the IFT dynein complex was examined in the *IFT140*^{RNAi} mutant. The IFT140 protein (also known as CHE11) is central to the formation of the IFT-A complex (Mukhopadhyay *et al.*, 2010; Behal *et al.*, 2012), and its absence results in the formation of short cilia or flagella filled with IFT particles (Qin *et al.*, 2001; Absalon *et al.*, 2008a). The penetrance of the phenotype was confirmed by IFA (Supplemental Figure S6). First, the total amount of DHC2.1 was analyzed by Western blot, showing that depletion of IFT140 did not visibly modify the quantity of DHC2.1 (Figure 10A). Second, GFP::DHC2.1, GFP::DLI1, and GFP::DIC5 were expressed in the *IFT140*^{RNAi} strain. In noninduced cells, all IFT dyneins displayed the typical distribution in the flagellum, at its base, and in the cytoplasm. In the *IFT140*^{RNAi} mutant, cells assembled short flagella filled with IFT protein, as confirmed by staining with the Mab25 axoneme marker and by the anti-IFT172 marker (Figure 10B). In these conditions, all IFT dynein subunits were concentrated at the flagellar base, producing a very bright signal (Figure 10, B and C). The cytoplasmic signal was depleted, and the short flagella looked totally negative. Triple staining showed

that dyneins were found in a compartment above the basal body marker Mab22 (unpublished data) but below the short axoneme stained with Mab25, whereas the IFT172 marker was found even further toward the far end of the dilated short flagellum (Figure 10B, inset). We conclude that the IFT dynein components are targeted normally to the flagellar base but fail to enter the flagellar compartment in the *IFT140*^{RNAi} mutant. This suggests that the IFT-A complex is involved in penetration of the IFT dynein in the flagellum, possibly by driving association to IFT trains or the IFT-B complex or by contributing to the passage through the transition zone.

DISCUSSION

A motile heterodimer of dynein heavy chains

To our knowledge, this is the first evidence in any eukaryote for the existence of a heterodimer of dynein heavy chains able to move along microtubules. So far, all reported cytoplasmic and IFT dynein complexes function as homodimers of heavy chains (Vale, 2003; Hom *et al.*, 2011; Schiavo *et al.*, 2013). Heterodimers (or even heterotrimers) of dynein heavy chains are active in the axoneme but are attached on microtubule doublets and do not proceed along them as does the IFT dynein (DiBella and King, 2001). The existence of a heterodimer of the nonmotor dynein chain Roadblock has been reported in mammals. This could contribute to enlarge the repertoire of dynein complexes available in the cytoplasm (Nikulina *et al.*, 2004). Strictly speaking, the existence of homodimers of DHC2.1 or DHC2.2 in *T. brucei* cannot be ruled out. However, several

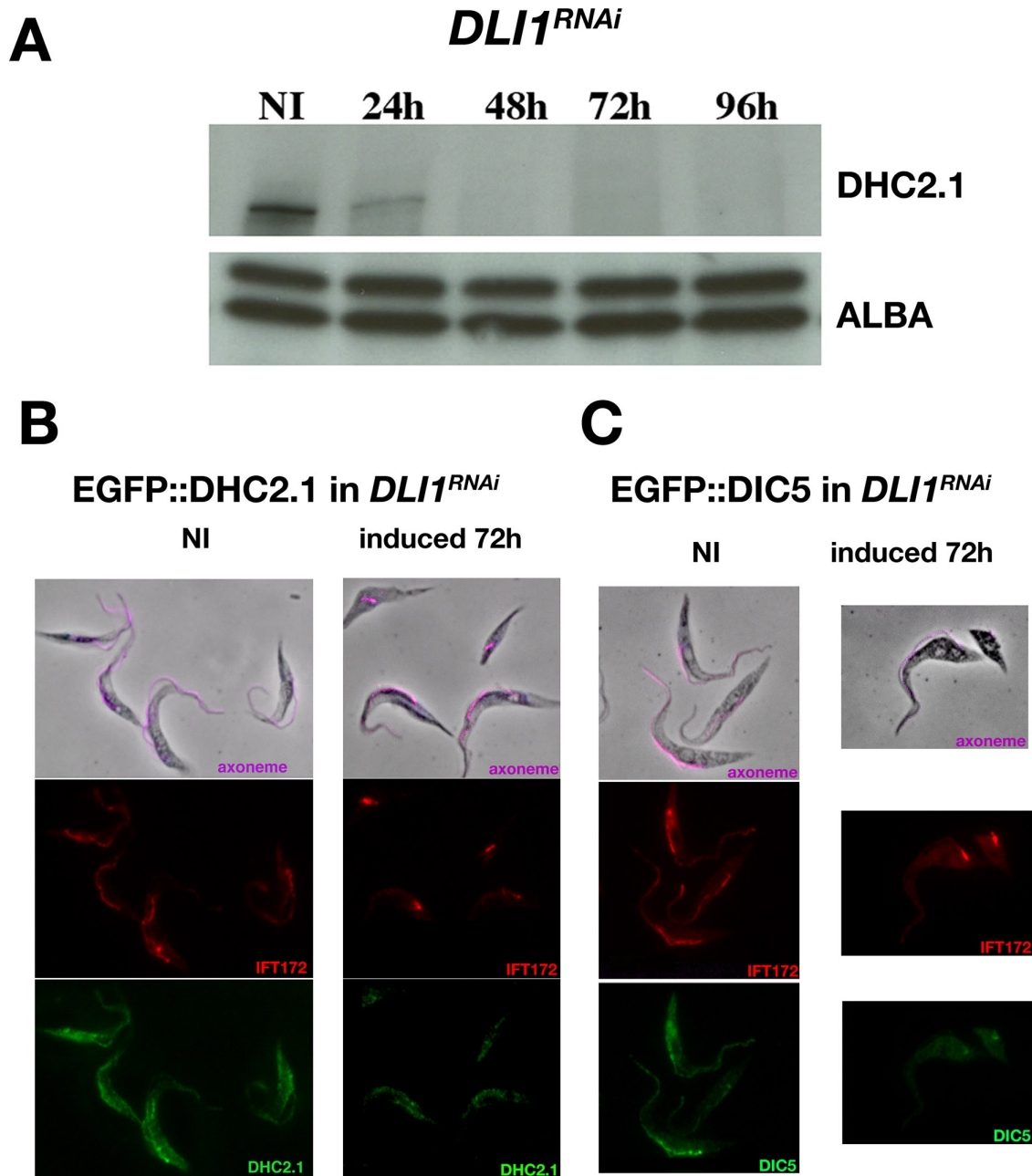


FIGURE 8: DLI1 is required for stability of the dynein heavy chains. (A) Western blot showing rapid loss of DHC2.1 during the course of RNAi silencing of DLI1. Cells were grown in the presence of tetracycline for the indicated periods of time. Total protein samples were separated by SDS-PAGE, blotted to a PVDF membrane, and incubated with the anti-DHC2.1 antibody. The anti-ALBA antibody was used as a loading control. (B, C) *DLI1*^{RNAi} cells expressing EGFP::DHC2.1 (B) or EGFP::DIC5 (C) were noninduced or grown in tetracycline for 72 h and stained with the axoneme marker Mab25 (red) and the anti-GFP (green). Both dynein chains are found in the flagellum, at the flagellar base, and in the cytoplasm in control cells, but their amount drops significantly in the *DLI1*^{RNAi} mutant. They are not found in the short flagellum.

arguments do not support their existence. First, knocking down any single DHC2 is sufficient to inhibit retrograde IFT and block normal flagellum formation. There is therefore no redundancy as observed for other duplicated genes in *T. brucei* (Dawe *et al.*, 2005). Second, trafficking of GFP::DHC2.1 is no longer detected as soon as DHC2.2 is silenced. Third, the absence of one dynein heavy chain leads to the rapid loss of the other one, supporting the view that they exist mostly as partners and not as single homodimeric entities.

The duplication of the *DHC2* genes must be ancient, as it is found in all species of kinetoplastids for which a genome is avail-

able: *T. congolense*, *T. vivax*, *T. cruzi*, all subspecies of *Leishmania*, and even the free-living *Bodo saltans* (Jackson *et al.*, 2008), excluding an association to parasitism. The evolutionary advantages of such a heterodimeric configuration remain to be established, but it could be related to the specific organization of the trypanosome flagellum (presence of a paraflagellar rod and an attachment region; Kohl and Bastin, 2005; Ralston *et al.*, 2009). Alternatively, the reason could be sought in the unusually fast IFT retrograde rate in trypanosomes, which can be up to 7 $\mu\text{m/s}$, compared with <4 $\mu\text{m/s}$ in other systems (Buisson *et al.*, 2013).

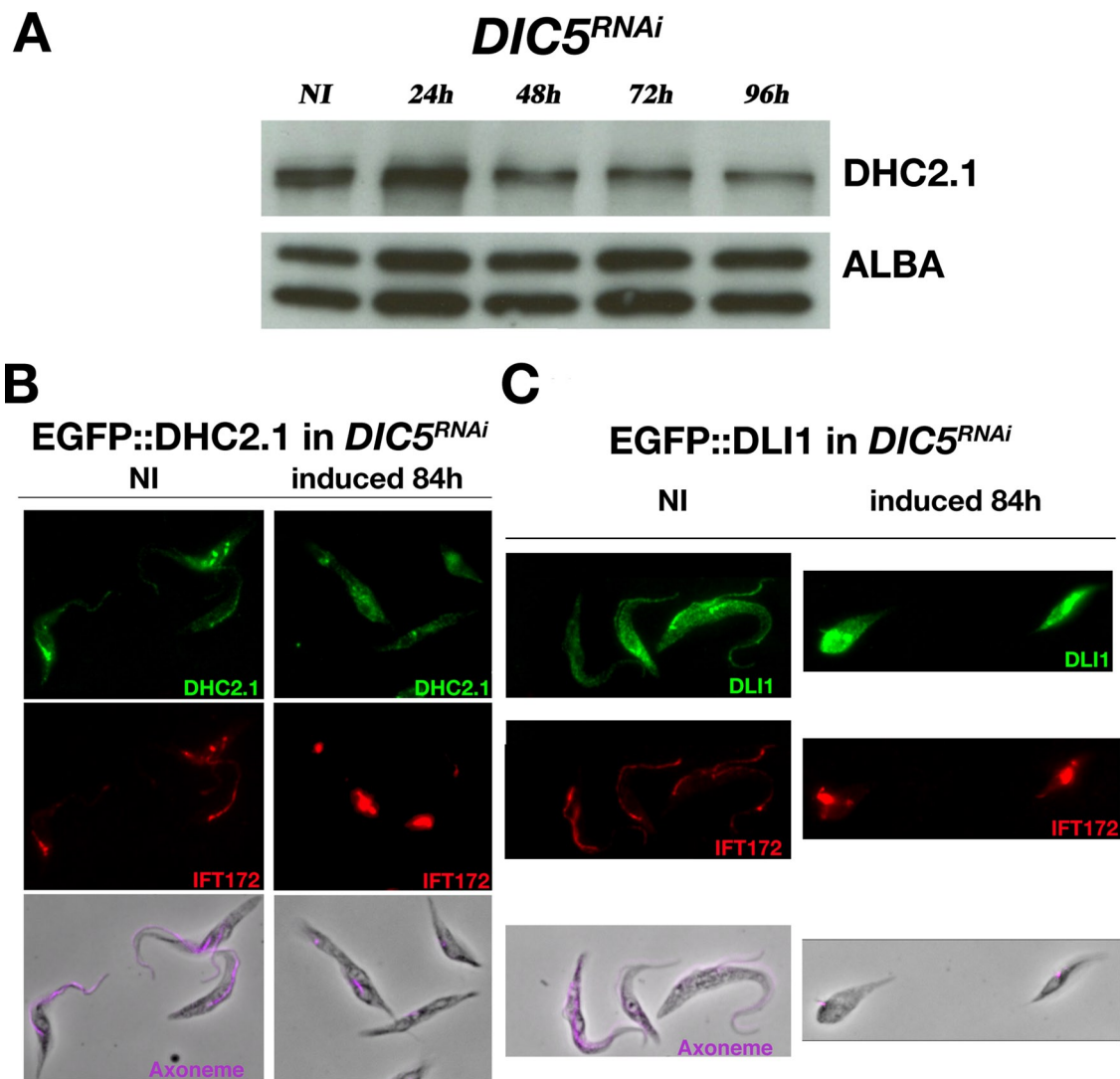


FIGURE 9: DIC5 is required for targeting the dynein complex to the base of the flagellum. (A) Western blot showing that the amounts of DHC2.1 were slightly affected during the course of RNAi silencing of DIC5. Cells were grown in the presence of tetracycline for the indicated periods of time. Total protein samples were separated by SDS-PAGE, blotted to a PVDF membrane, and incubated with the anti-DHC2.1 antibody. The anti-ALBA antibody was used as a loading control. (B, C) *DIC5*^{RNAi} cells expressing EGFP::DHC2.1 (B) or EGFP::DLI1 (C) were noninduced or grown in tetracycline for 84 h and stained with the axoneme marker Mab25 (red) and the anti-GFP (green). Both dynein chains are found in the flagellum, at the flagellar base, and in the cytoplasm in control cells but are dispersed in the cytoplasm in the *DIC5*^{RNAi} mutant. They are not found in the short flagellum.

A model for IFT dynein formation and function in retrograde transport

On the basis of the results reported here and existing literature, we propose a model to explain the contributions of different partners to retrograde transport (Figure 11). The IFT dynein complex is composed of at least five proteins: a dimer of heavy dynein chain (a homodimer or a heterodimer, as reported here for *T. brucei*), two distinct intermediate chains (DIC5/FAP133 and FAP163/WD60), a light IC (D1bLIC or XBX1), and a light chain (LC8; Pazour *et al.*, 1998, 1999; Signor *et al.*, 1999; Schafer *et al.*, 2003; Hou *et al.*, 2004; Rompolas *et al.*, 2007; Patel-King *et al.*, 2013). This complex would be assembled in the cytoplasm independently of IFT proteins, as shown by the presence of the usual amount and normal targeting of all dynein members at the flagellar base in the *IFT140*^{RNAi} mutant. The assembly machinery of the IFT dynein must be distinct from that used for outer dynein arm assembly, since interfering with the latter

inhibits formation of axonemal dynein arms but does not perturb flagellum elongation (Omran *et al.*, 2008; Duquesnoy *et al.*, 2009).

Heavy chains and the light IC appear essential for the formation and/or stability of the IFT dynein complex or its individual components. When one of these components is depleted, the abundance of the other partners drops and they appear dispersed in the cytoplasm, with little or no material at the flagellar base or within the flagellum. This is supported by analysis of *Chlamydomonas* mutants lacking either DHC2 or DLI1: the amount of each partner is significantly reduced in the absence of the other one (Hou *et al.*, 2004; Morga and Bastin, 2013).

After assembly, the IFT dynein complex needs to reach the flagellar base, a process that takes place less efficiently in the *DIC5*^{RNAi} mutant. DIC5 was identified in a comparative genomic screen for proteins conserved only in species with motile cilia (Baron *et al.*, 2007). Its RNAi knockdown in *T. brucei* resulted in reduced motility,

WT+ <i>GFP::DHC2.1</i>
WT+ <i>GFP::DHC2.2</i>
WT+ <i>GFP::DLI1</i>
WT+ <i>GFP::DIC5</i>
<i>DHC2.1^{RNAi}</i>
<i>DHC2.1^{RNAi} + GFP::DHC2.2</i>
<i>DHC2.1^{RNAi} + GFP::DHC2.1</i>
<i>DHC2.1^{RNAi} + GFP::DLI1</i>
<i>DHC2.1^{RNAi} + GFP::DIC5</i>
<i>DHC2.2^{RNAi}</i>
<i>DHC2.2^{RNAi} + GFP::DHC2.1</i>
<i>DLI1^{RNAi}</i>
<i>DLI1^{RNAi} + GFP::DHC2.1</i>
<i>DLI1^{RNAi} + GFP::DIC5</i>
<i>DIC5^{RNAi}</i>
<i>DIC5^{RNAi} + GFP::DHC2.1</i>
<i>DIC5^{RNAi} + GFP::DLI1</i>
<i>IFT140^{RNAi}</i>
<i>IFT140^{RNAi} + GFP::DHC2.1</i>
<i>IFT140^{RNAi} + GFP::DLI1</i>
<i>IFT140^{RNAi} + GFP::DIC5</i>

TABLE 1: Strains used in this study.

but the phenotype was not analyzed further (Baron et al., 2007). In zebrafish, reducing the expression of DIC5 by the injection of morpholino oligonucleotides interfered with cilia formation in eye and kidney (Krock et al., 2009), a phenomenon also reported in mammalian cells upon small interfering RNA transfection (Asante et al., 2013). In the induced *DIC5^{RNAi}* cell line, the amounts of heavy and light intermediate chains are slightly reduced, but their distribution is significantly affected, with greatly reduced concentration at the flagellar base and more-dispersed localization in the cell body. The mechanism by which the IFT dynein complex reaches the flagellar base remains open to discussion: it could be an active process—for example, by migration along cytoplasmic microtubules whose minus ends are found close to the basal body—or it could rely on cytoplasmic diffusion followed by retention at the flagellar base. Because of its multiple WD domains, DIC5 could interact with different partners, such as proteins involved in vesicular trafficking, and hence participate in flagellum targeting (Jekely and Arendt, 2006). Clear homologues of DIC5/FAP133 and of the other intermediate dynein chain, WD60/FAP163, could not be identified in *C. elegans* (Rompolas et al., 2007; Patel-King et al., 2013). This amazing absence might reflect a different mode of ciliary trafficking associated with the peculiar organization of the ciliary base in this organism (Hao et al., 2011; Williams et al., 2011; Doroquez et al., 2014).

Once the IFT dynein complex has reached the flagellar base, it still needs to access the flagellar compartment and go across the

ciliary pore complex. This process could be correlated with the presence of the IFT-A complex, another important actor in retrograde transport. Interfering with any of its six members produces phenotypes very similar to those observed upon IFT dynein inhibition in nematodes (Perkins et al., 1986), green algae (Iomini et al., 2009), trypanosomes (Absalon et al., 2008b), or mammals (Perrault et al., 2012). It is often assumed that IFT-A and IFT-dynein interact to drive retrograde transport, but evidence for direct interactions is scarce (Rompolas et al., 2007). The IFT-A complex could be essential to retrograde transport by different means: it could function as a bridge between the dynein motor and the IFT-B complex during anterograde transport, it could control motor transition between kinesin and dynein at the distal tip, or it could be responsible for access of the IFT dynein to the flagellum. In all cases, its malfunctioning would perturb retrograde transport. In *T. brucei*, all four dynein subunits investigated here are jammed at the flagellar base in the *IFT140^{RNAi}* mutant and not encountered in the flagellum. A similar situation was reported for D1bLIC/XBX1 in the *C. elegans che-11* mutant (the homologue of IFT140), although some transport could still be detected in the cilium (Schafer et al., 2003), perhaps because the penetrance of the IFT-A mutations in nematodes is weaker than what is observed for trypanosomes (Blacque et al., 2006; Absalon et al., 2008b; Adhiambo et al., 2009). We propose that the IFT-A complex is required for efficient entry of the IFT dynein in the flagellar compartment. This could be achieved by docking to the IFT-B complex or to the IFT kinesin 2, as observed in *Chlamydomonas* using immunoprecipitation techniques (Pedersen et al., 2006). Alternatively, the IFT-A complex could function as an adapter to allow the passage of the transition zone. In this case, interactions between IFT-A and IFT dynein proteins would be transient, hence explaining the low amount of copurified material reported so far (Rompolas et al., 2007). Such interaction could be favored by the high local concentration of IFT material encountered at the flagellar base (Morga and Bastin, 2013), possibly explaining why IFT has only been reported in the flagellum, despite the presence of large amounts of IFT material in the cytoplasm (Ahmed et al., 2008; Wang et al., 2009). Understanding how IFT complexes and IFT motors interact at the base of the flagellum to ensure formation of anterograde trains and recycling of retrograde trains will be the next challenge.

MATERIALS AND METHODS

Trypanosome cell lines and cultures

All cell lines used for this work were derivatives of strain 427 of *T. brucei* and cultured in SDM79 medium supplemented with hemin and 10% fetal calf serum. The cell line *DHC2.2^{RNAi}* has been described previously (Kohl et al., 2003). It expresses complementary single-stranded RNA corresponding to a fragment of the gene of interest from two tetracycline-inducible T7 promoters facing each other in the pZJM vector (Wang et al., 2000) transformed in 29-13 cells that express the T7 RNA polymerase and the tetracycline repressor (Wirtz et al., 1999). Addition of tetracycline (1 µg/ml) to the medium induces expression of sense and anti-sense RNA strands that can anneal to form double-stranded RNA (dsRNA) and trigger RNAi.

Plasmid construction and transformation in trypanosomes

For generation of cell lines expressing dsRNA for RNAi knockdown, sequences were selected according to their lack of significant identity with other genes to avoid cross-RNAi (Durand-Dubief et al., 2003) using the RNAit algorithm (Redmond et al., 2003). Primers are available on request from the authors. Gene fragments were amplified by PCR on *T. brucei* genomic DNA, purified on QIA-Quick

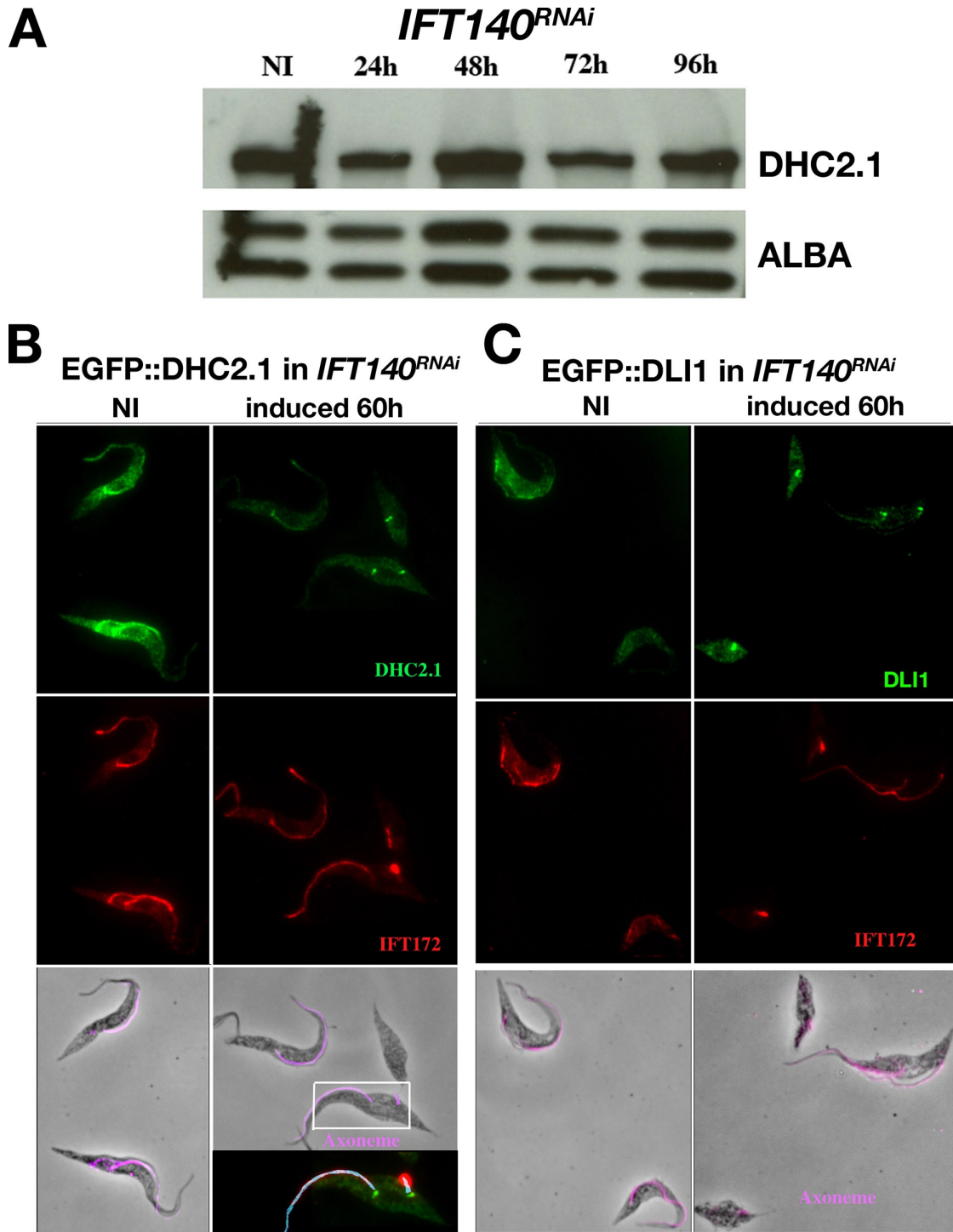


FIGURE 10: The IFT-A IFT140 protein is required for entry of the IFT dynein complex in the flagellum. (A) Western blot showing that the amounts of DHC2.1 are not modified during the course of RNAi silencing of IFT140. Cells were grown in the presence of tetracycline for the indicated periods of time. Total protein samples were separated by SDS-PAGE, blotted to a PVDF membrane, and incubated with the anti-DHC2.1 antibody. The anti-ALBA antibody was used as a loading control. (B, C) *IFT140*^{RNAi} cells expressing EGFP::DHC2.1 (B) or EGFP::DLI1 (C) were noninduced or grown in tetracycline for 60 h and stained with the axoneme marker Mab25 (red) and the anti-GFP (green). Both dynein chains are found in the flagellum, at the flagellar base, and in the cytoplasm in control cells but are concentrated at the base of the short flagellum in the *IFT140*^{RNAi} mutant. They are not found in the short flagellum. The magnified area shows the base of a short flagellum. The GFP signal for the GFP::DHC2.1 fusion is found well below the axoneme, presumably at the level of the transition zone, whereas the accumulated IFT172 material (green) is found at the distal end of the flagellum.

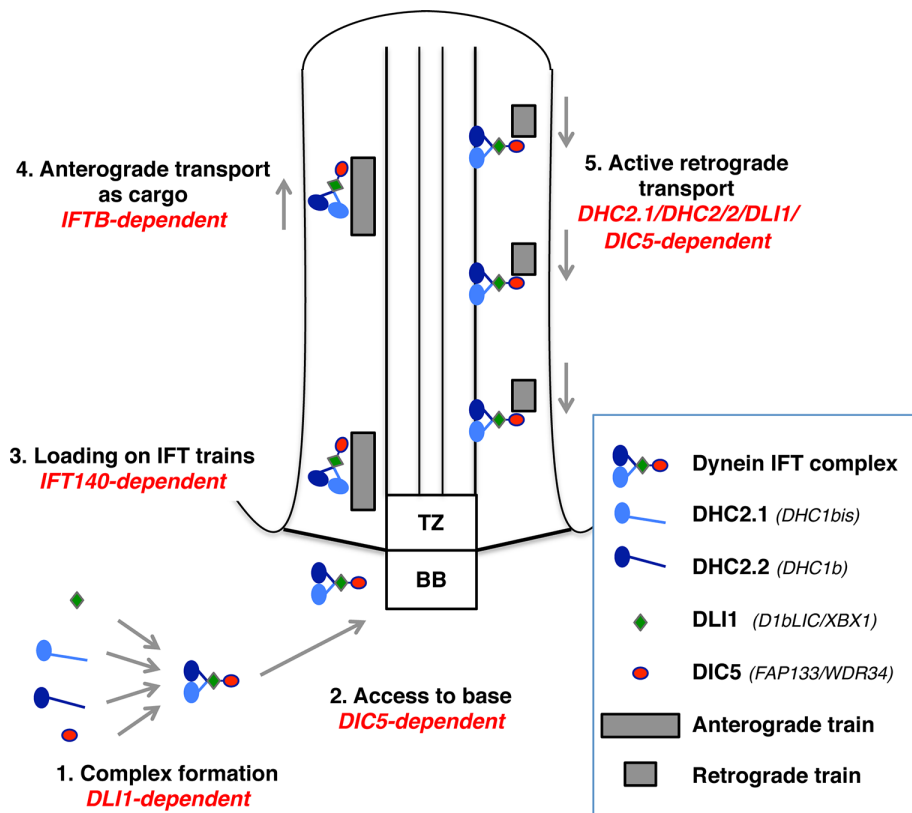


FIGURE 11: Molecular model for IFT dynein complex formation and function. The dependence on specific molecules is indicated in red for each step. 1) Dynein subunits are assembled in the cytoplasm to form the dynein complex. This step relies on all four subunits but more specifically on DLI1. 2) The IFT dynein complex reaches the base of the flagellum. This step depends on the presence of DIC5. 3) The dynein complex is loaded on IFT trains in an IFT140 (or the full IFT-A complex)–dependent manner. 4) The dynein complex is a cargo of the anterograde train and is transported to the tip of the axoneme. This relies on anterograde transport and hence on IFT-B and kinesin motor (not drawn here). 5) The short retrograde trains are returned to the base of the flagellum. An intact IFT dynein complex is required, since the depletion of any of its components is sufficient to abolish retrograde IFT. Not drawn to scale. The space between the microtubules and the membrane has been enlarged to facilitate representation of IFT trains. BB, basal body; TZ, transition zone.

columns (Qiagen), digested with *HindIII* and *XhoI*, and ligated in the corresponding sites of the pZJM vector. For expression of dynein subunits fused to EGFP, the 5' end of each gene was amplified by PCR from genomic DNA and cut by the *NheI* and *BamHI* enzymes for ligation in the *NheI* and *BamHI* sites of the pCPFRGFP vector (Adhiambo *et al.*, 2009). All inserted sequences and flanking regions were sequenced to confirm correct integration and fusion.

For transfection, pZJM plasmids were linearized with *NotI* for transformation in 29-13 cells upon integration in the rDNA locus. For endogenous tagging, each pCPFRGFP construct was linearized with a specific enzyme allowing recombination within the *DHC2.1* (*MfeI*), *DHC2.2* (*NcoI*), *DLI1* (*MunI*), or *DIC5* (*XhoI*) gene. Cells were transfected by nucleofection (Amaxa). In all cases, transfected cells were immediately cloned, and all antibiotic-resistant cell lines were characterized either by direct observation by phase contrast to detect cells with defective flagellum assembly or by direct fluorescence observation (GFP). The list of strains constructed for this project is given in Table 1. RNAi was induced by addition of 1 μ g tetracycline/ml of medium, and fresh tetracycline was added at each cell dilution. Cell culture growth was monitored daily with an automatic Z2 cell counter (Beckman Coulter, Villepinte, France).

Protein expression and antibody production

Given their large size and the close similarity of their central portion, only a fragment of DHC2.1 and DHC2.2 was cloned and expressed in *Escherichia coli*, using the pGEXB vector for protein expression. The plasmids were sequenced to confirm identity and correct fusion with glutathione *S*-transferase (GST). Plasmids were transformed in the competent BL21 strain of *E. coli*, and protein expression was analyzed by SDS–PAGE followed by Coomassie staining. The domains expressed are from aa 323–488 for DHC2.1 and 308–509 for DHC2.2. GST-coupled proteins were purified as described (Smith and Johnson, 1988) and injected into BALB/C mice for immunization. After bleeding, sera were absorbed against GST. Sera from mice immunized with GST alone were used as negative controls.

Immunofluorescence and light microscopy analysis

For immunofluorescence, cells were washed in SDM79 medium without serum, settled on poly-L-lysine-coated slides, and fixed in methanol for a maximum of 5 min at -20°C . Slides were incubated with 1:200 dilution of antiserum for 45–60 min in phosphate-buffered saline (PBS)–bovine serum albumin 0.1%. Slides were washed in PBS and incubated with the appropriate anti-mouse secondary antibodies coupled to various fluorophores (Invitrogen, Carlsbad, CA). The monoclonal antibody Mab25 (immunoglobulin G2a [IgG2a]; Pradel *et al.*, 2006), which specifically recognizes the axoneme protein TbSAXO1 (Dacheux *et al.*, 2012), was used as marker of flagellum assembly. The monoclonal antibody MAb22 is an IgM that detects an as-yet-unidentified antigen found at the proximal zone of both the mature and the probasal body (Bonhivers *et al.*, 2008).

GFP was observed directly or upon fixation by immunofluorescence using a 1:500 dilution of a rabbit anti-GFP antibody (Invitrogen). The mouse anti-DHC2.1 and anti-DHC2.2 antibodies were used at a 1:100 dilution. Subclass-specific secondary antibodies coupled to fluorescein isothiocyanate (Sigma-Aldrich, St. Louis, MO), Alexa 488 or Alexa 594 (Invitrogen), and Cy3 or Cy5 (Jackson ImmunoResearch, West Grove, PA) were used for double or triple labeling. Slides were stained with 4',6-diamidino-2-phenylindole (DAPI) for visualization of kinetoplast and nuclear DNA content. Samples were observed with a DMI4000 Leica microscope, and images were acquired with a Retiga-SRV (Q-Imaging, Surrey, Canada) or a Horca 03G (Hamamatsu, Hamamatsu City, Japan) camera. Images were analyzed using ImageJ (National Institutes of Health, Bethesda, MD). In the case of RNAi mutants, IFA signals were normalized using the signal obtained in non-induced controls as a reference.

For visualization of GFP on live cells, trypanosomes were treated as described (Buisson *et al.*, 2013). For IFT quantification, a Zeiss inverted microscope (Axiovert 200; Jena, Germany) equipped with

an oil immersion objective (magnification 63× with numerical aperture 1.4) and a spinning disk confocal head (CSU22; Yokogawa, Tokyo, Japan) were used. Images were acquired using Velocity software with an electron-multiplying charge-coupled device camera (C-9100; Hamamatsu) operating in streaming mode. A sample of cell (a 100- μ l drop) was taken directly from the culture grown at (6–8) $\times 10^6$ cells/ml and trapped between slide and coverslip. The samples were kept at 27°C using a temperature-controlled chamber. The samples were used no longer than 30 min. For kymograph analysis, anterograde and retrograde transports were separately extracted and quantified as previously described (Chenouard *et al.*, 2010; Buisson *et al.*, 2013).

Electron microscopy

Fixation, embedding, and sectioning for transmission electron microscopy were carried out as described previously (Absalon *et al.*, 2008a). For scanning electron microscopy, cells were washed in PBS, fixed with 2.5% glutaraldehyde, and treated as reported previously (Absalon *et al.*, 2007).

Western blot

Cells were washed in PBS, homogenized, and boiled in gel sample buffer before SDS-PAGE. Proteins were transferred to polyvinylidene fluoride (PVDF) membranes that were blocked with 5% milk and probed with an anti-GFP antibody (1:800 dilution; Roche), or with the anti-DHC2.1 (1:100) or the anti-DHC2.2 (1:100). The anti-ALBA (dilution 1:1000; Subota *et al.*, 2011) or the anti-PFR antibody L13D6 (dilution 1:50; Kohl *et al.*, 1999) served as loading control. Bound antibodies were revealed with ECL+ (Amersham).

ACKNOWLEDGMENTS

We acknowledge Derrick Robinson (University of Bordeaux 2, Bordeaux, France) for the generous gift of monoclonal antibodies and Brice Rotureau for critical reading of the manuscript. J.B. and S.A. were funded by MNRT (French Ministry of Research), the Fondation pour la Recherche Médicale, and Pasteur–Weizmann predoctoral fellowships. This work was funded by the Institut Pasteur, the Centre National de la Recherche Scientifique, and grants ANR-09-GENO-022-03 and ANR-11-BSV8-016-03 from the French National Research Agency.

REFERENCES

Absalon S, Blisnick T, Bonhivers M, Kohl L, Cayet N, Toutirais G, Buisson J, Robinson D, Bastin P (2008a). Flagellum elongation is required for correct structure, orientation and function of the flagellar pocket in *Trypanosoma brucei*. *J Cell Sci* 121, 3704–3716.

Absalon S, Blisnick T, Kohl L, Toutirais G, Dore G, Julkowska D, Tavenet A, Bastin P (2008b). Intraflagellar transport and functional analysis of genes required for flagellum formation in trypanosomes. *Mol Biol Cell* 19, 929–944.

Absalon S, Kohl L, Branche C, Blisnick T, Toutirais G, Rusconi F, Cosson J, Bonhivers M, Robinson D, Bastin P (2007). Basal body positioning is controlled by flagellum formation in *Trypanosoma brucei*. *PLoS One* 2, e437.

Adhiambo C, Blisnick T, Toutirais G, Delannoy E, Bastin P (2009). A novel function for the atypical small G protein Rab-like 5 in the assembly of the trypanosome flagellum. *J Cell Sci* 122, 834–841.

Adhiambo C, Forney JD, Asai DJ, LeBowitz JH (2005). The two cytoplasmic dynein-2 isoforms in *Leishmania mexicana* perform separate functions. *Mol Biochem Parasitol* 143, 216–225.

Ahmed NT, Gao C, Lucker BF, Cole DG, Mitchell DR (2008). ODA16 aids axonemal outer row dynein assembly through an interaction with the intraflagellar transport machinery. *J Cell Biol* 183, 313–322.

Arts HH, Bongers EM, Mans DA, van Beersum SE, Oud MM, Bolat E, Spruijt L, Cornelissen EA, Schuurs-Hoeijmakers JH, de Leeuw N, *et al.* (2011). C14ORF179 encoding IFT43 is mutated in Sensenbrenner syndrome. *J Med Genet* 48, 390–395.

Asante D, Maccarthy-Morrogh L, Townley AK, Weiss MA, Katayama K, Palmer KJ, Suzuki H, Westlake CJ, Stephens DJ (2013). A role for the Golgi matrix protein giantin in cillogenesis through control of the localization of dynein-2. *J Cell Sci* 126, 5189–5197.

Baron DM, Ralston KS, Kabututu ZP, Hill KL (2007). Functional genomics in *Trypanosoma brucei* identifies evolutionarily conserved components of motile flagella. *J Cell Sci* 120, 478–491.

Behal RH, Miller MS, Qin H, Lucker BF, Jones A, Cole DG (2012). Subunit interactions and organization of the *Chlamydomonas reinhardtii* intraflagellar transport complex A proteins. *J Biol Chem* 287, 11689–11703.

Berriman M, Ghedin E, Hertz-Fowler C, Blandin G, Renauld H, Bartholomeu DC, Lennard NJ, Caler E, Hamlin NE, Haas B, *et al.* (2005). The genome of the African trypanosome *Trypanosoma brucei*. *Science* 309, 416–422.

Bhogaraju S, Cajanek L, Fort C, Blisnick T, Weber K, Taschner M, Mizuno N, Lamla S, Bastin P, Nigg EA, *et al.* (2013a). Molecular basis of tubulin transport within the cilium by IFT74 and IFT81. *Science* 341, 1009–1012.

Bhogaraju S, Engel BD, Lorentzen E (2013b). Intraflagellar transport complex structure and cargo interactions. *Cilia* 2, 10.

Blacque OE, Li C, Inglis PN, Esmail MA, Ou G, Mah AK, Baillie DL, Scholey JM, Leroux MR (2006). The WD repeat-containing protein IFTA-1 is required for retrograde intraflagellar transport. *Mol Biol Cell* 17, 5053–5062.

Bonhivers M, Landrein N, Decossas M, Robinson DR (2008). A monoclonal antibody marker for the exclusion-zone filaments of *Trypanosoma brucei*. *Parasit Vectors* 1, 21.

Bredrup C, Saunier S, Oud MM, Fiskerstrand T, Hoischen A, Brackman D, Leh SM, Midtbo M, Filhol E, Bole-Feysot C, *et al.* (2011). Ciliopathies with skeletal anomalies and renal insufficiency due to mutations in the IFT-A gene WDR19. *Am J Hum Gen* 89, 634–643.

Briggs LJ, Davidge JA, Wickstead B, Ginger ML, Gull K (2004). More than one way to build a flagellum: comparative genomics of parasitic protozoa. *Curr Biol* 14, R611–612.

Buisson J, Chenouard N, Lagache T, Blisnick T, Olivo-Marin JC, Bastin P (2013). Intraflagellar transport proteins cycle between the flagellum and its base. *J Cell Sci* 126, 327–338.

Chenouard N, Buisson J, Bloch I, Bastin P, Olivo-Marin JC (2010). Curvelet analysis of kymograph for tracking bi-directional particles in fluorescence microscopy images. In: 17th IEEE International Conference on Image Processing, Piscataway, NJ: IEEE, 3657–3660.

Dacheux D, Landrein N, Thonnus M, Gilbert G, Sahin A, Wodrich H, Robinson DR, Bonhivers M (2012). A MAP6-related protein is present in protozoa and is involved in flagellum motility. *PLoS One* 7, e31344.

Dagoneau N, Goulet M, Genevieve D, Sznajder Y, Martinovic J, Smithson S, Huber C, Baujat G, Flori E, Tecco L, *et al.* (2009). DYNC2H1 mutations cause asphyxiating thoracic dystrophy and short rib-polydactyly syndrome, type III. *Am J Hum Gen* 84, 706–711.

Davis EE, Zhang Q, Liu Q, Diplas BH, Davey LM, Hartley J, Stoetzel C, Szymanska K, Ramaswami G, Logan CV, *et al.* (2011). TTC21B contributes both causal and modifying alleles across the ciliopathy spectrum. *Nat Genet* 43, 189–196.

Dawe HR, Farr H, Portman N, Shaw MK, Gull K (2005). The Parkin co-regulated gene product, PACRG, is an evolutionarily conserved axonemal protein that functions in outer-doublet microtubule morphogenesis. *J Cell Sci* 118, 5421–5430.

DiBella LM, King SM (2001). Dynein motors of the *Chlamydomonas* flagellum. *Int Rev Cytol* 210, 227–268.

Doroquez DB, Berciu C, Anderson JR, Sengupta P, Nicastro D (2014). A high-resolution morphological and ultrastructural map of anterior sensory cilia and glia in *Caenorhabditis elegans*. *eLife* 3, e01948.

Duquesnoy P, Escudier E, Vincensini L, Freshour J, Bridoux AM, Coste A, Deschildre A, de Blic J, Legendre M, Montantin G, *et al.* (2009). Loss-of-function mutations in the human ortholog of *Chlamydomonas reinhardtii* ODA7 disrupt dynein arm assembly and cause primary ciliary dyskinesia. *Am J Hum Gen* 85, 890–896.

Durand-Dubief M, Kohl L, Bastin P (2003). Efficiency and specificity of RNA interference generated by intra- and intermolecular double stranded RNA in *Trypanosoma brucei*. *Mol Biochem Parasitol* 129, 11–21.

Finn RD, Bateman A, Clements J, Coggill P, Eberhardt RY, Eddy SR, Heger A, Hetherington K, Holm L, Mistry J, *et al.* (2014). Pfam: the protein families database. *Nucleic Acids Res* 42, D222–230.

Franklin JB, Ullu E (2010). Biochemical analysis of PIFTC3, the *Trypanosoma brucei* orthologue of nematode DYF-13, reveals interactions with established and putative intraflagellar transport components. *Mol Microbiol* 78, 173–186.

Gilissen C, Arts HH, Hoischen A, Spruijt L, Mans DA, Arts P, van Lier B, Steehouwer M, van Reeuwijk J, Kant SG, *et al.* (2010). Exome

- sequencing identifies WDR35 variants involved in Sensenbrenner syndrome. *Am J Hum Gen* 87, 418–423.
- Hao L, Efimenko E, Swoboda P, Scholey JM (2011). The retrograde IFT machinery of *C. elegans* cilia: two IFT dynein complexes? *PLoS one* 6, e20995.
- Hom EF, Witman GB, Harris EH, Dutcher SK, Kamiya R, Mitchell DR, Pazour GJ, Porter ME, Sale WS, Wirschell M, et al. (2011). A unified taxonomy for ciliary dyneins. *Cytoskeleton (Hoboken)* 68, 555–565.
- Hou Y, Pazour GJ, Witman GB (2004). A dynein light intermediate chain, D1bLIC, is required for retrograde intraflagellar transport. *Mol Biol Cell* 15, 4382–4394.
- Huber C, Wu S, Kim AS, Sigaudy S, Sarukhanov A, Serre V, Baujat G, Le Quan Sang KH, Rimoin DL, Cohn DH, et al. (2013). WDR34 mutations that cause short-rib polydactyly syndrome type III/severe asphyxiating thoracic dysplasia reveal a role for the NF-kappaB pathway in cilia. *Am J Hum Gen* 93, 926–931.
- Huet D, Blisnick T, Perrot S, Bastin P (2014). The GTPase IFT27 is involved in both anterograde and retrograde intraflagellar transport. *eLife* 3, e02419.
- Iomini C, Li L, Esparza JM, Dutcher SK (2009). Retrograde intraflagellar transport mutants identify complex A proteins with multiple genetic interactions in *Chlamydomonas reinhardtii*. *Genetics* 183, 885–896.
- Jackson AP, Quail MA, Berriman M (2008). Insights into the genome sequence of a free-living kinetoplastid: *Bodo saltans* (Kinetoplastida: Euglenozoa). *BMC Genomics* 9, 594.
- Jekely G, Arendt D (2006). Evolution of intraflagellar transport from coated vesicles and autogenous origin of the eukaryotic cilium *BioEssays* 28, 191–198.
- Kohl L, Bastin P (2005). The flagellum of trypanosomes. *Int Rev Cytol* 244, 227–285.
- Kohl L, Robinson D, Bastin P (2003). Novel roles for the flagellum in cell morphogenesis and cytokinesis of trypanosomes. *EMBO J* 22, 5336–5346.
- Kohl L, Sherwin T, Gull K (1999). Assembly of the paraflagellar rod and the flagellum attachment zone complex during the *Trypanosoma brucei* cell cycle. *J Eukaryot Microbiol* 46, 105–109.
- Kozminski KG, Johnson KA, Forscher P, Rosenbaum JL (1993). A motility in the eukaryotic flagellum unrelated to flagellar beating. *Proc Natl Acad Sci USA* 90, 5519–5523.
- Krock BL, Mills-Henry I, Perkins BD (2009). Retrograde intraflagellar transport by cytoplasmic dynein-2 is required for outer segment extension in vertebrate photoreceptors but not arrestin translocation. *Invest Ophthalmol Vis Sci* 50, 5463–5471.
- Morga B, Bastin P (2013). Getting to the heart of intraflagellar transport using *Trypanosoma* and *Chlamydomonas* models: the strength is in their differences. *Cilia* 2, 16.
- Mukhopadhyay S, Wen X, Chih B, Nelson CD, Lane WS, Scales SJ, Jackson PK (2010). TULP3 bridges the IFT-A complex and membrane phosphoinositides to promote trafficking of G protein-coupled receptors into primary cilia. *Genes Dev* 24, 2180–2193.
- Nikulina K, Patel-King RS, Takebe S, Pfister KK, King SM (2004). The Roadblock light chains are ubiquitous components of cytoplasmic dynein that form homo- and heterodimers. *Cell Motil Cytoskeleton* 57, 233–245.
- Omran H, Kobayashi D, Olbrich H, Tsukahara T, Loges NT, Hagiwara H, Zhang Q, Leblond G, O'Toole E, Hara C, et al. (2008). Ktu/PF13 is required for cytoplasmic pre-assembly of axonemal dyneins. *Nature* 456, 611–616.
- Patel-King RS, Gilbert RM, Hom EF, King SM (2013). WD60/FAP163 is a dynein intermediate chain required for retrograde intraflagellar transport in cilia. *Mol Biol Cell* 24, 2668–2677.
- Pazour GJ, Dickert BL, Witman GB (1999). The DHC1b (DHC2) isoform of cytoplasmic dynein is required for flagellar assembly. *J Cell Biol* 144, 473–481.
- Pazour GJ, Wilkerson CG, Witman GB (1998). A dynein light chain is essential for the retrograde particle movement of intraflagellar transport (IFT). *J Cell Biol* 141, 979–992.
- Pedersen LB, Geimer S, Rosenbaum JL (2006). Dissecting the molecular mechanisms of intraflagellar transport in *Chlamydomonas*. *Curr Biol* 16, 450–459.
- Perkins LA, Hedgecock EM, Thomson JN, Culotti JG (1986). Mutant sensory cilia in the nematode *Caenorhabditis elegans*. *Dev Biol* 117, 456–487.
- Perrault I, Saunier S, Hanein S, Filhol E, Bizet AA, Collins F, Salihi MA, Gerber S, Delphin N, Bigot K, et al. (2012). Mainzer-Saldino syndrome is a ciliopathy caused by IFT140 mutations. *Am J Hum Gen* 90, 864–870.
- Porter ME, Bower R, Knott JA, Byrd P, Dentler W (1999). Cytoplasmic dynein heavy chain 1b is required for flagellar assembly in *Chlamydomonas*. *Mol Biol Cell* 10, 693–712.
- Pradel LC, Bonhivers M, Landrein N, Robinson DR (2006). NIMA-related kinase TbNRKC is involved in basal body separation in *Trypanosoma brucei*. *J Cell Sci* 119, 1852–1863.
- Qin H, Rosenbaum JL, Barr MM (2001). An autosomal recessive polycystic kidney disease gene homolog is involved in intraflagellar transport in *C. elegans* ciliated sensory neurons. *Curr Biol* 11, 457–461.
- Ralston KS, Kabututu ZP, Melehani JH, Oberholzer M, Hill KL (2009). The *Trypanosoma brucei* flagellum: moving parasites in new directions. *Annu Rev Microbiol* 63, 335–362.
- Redmond S, Vadivelu J, Field MC (2003). RNAi: an automated web-based tool for the selection of RNAi targets in *Trypanosoma brucei*. *Mol Biochem Parasitol* 128, 115–118.
- Rompolas P, Pedersen LB, Patel-King RS, King SM (2007). *Chlamydomonas* FAP133 is a dynein intermediate chain associated with the retrograde intraflagellar transport motor. *J Cell Sci* 120, 3653–3665.
- Rosenbaum JL, Witman GB (2002). Intraflagellar transport. *Nat Rev Mol Cell Biol* 3, 813–825.
- Sakato M, King SM (2004). Design and regulation of the AAA+ microtubule motor dynein. *J Struct Biol* 146, 58–71.
- Schafer JC, Haycraft CJ, Thomas JH, Yoder BK, Swoboda P (2003). XBX-1 encodes a dynein light intermediate chain required for retrograde intraflagellar transport and cilia assembly in *Caenorhabditis elegans*. *Mol Biol Cell* 14, 2057–2070.
- Schiavo G, Greensmith L, Hafezparast M, Fisher EM (2013). Cytoplasmic dynein heavy chain: the servant of many masters. *Trends Neurosci* 36, 641–651.
- Schmidts M, Vodopiu J, Christou-Savina S, Cortes CR, McInerney-Leo AM, Emes RD, Arts HH, Tuysuz B, D'Silva J, Leo PJ, et al. (2013). Mutations in the gene encoding IFT dynein complex component WDR34 cause Jeune asphyxiating thoracic dystrophy. *Am J Hum Gen* 93, 932–944.
- Scholey JM (2013). Kinesin-2: a family of heterotrimeric and homodimeric motors with diverse intracellular transport functions. *Annu Rev Cell Dev Biol* 29, 443–469.
- Signor D, Wedaman KP, Orozco JT, Dwyer ND, Bargmann CI, Rose LS, Scholey JM (1999). Role of a class DHC1b dynein in retrograde transport of IFT motors and IFT raft particles along cilia, but not dendrites, in chemosensory neurons of living *Caenorhabditis elegans*. *J Cell Biol* 147, 519–530.
- Smith DB, Johnson KS (1988). Single-step purification of polypeptides expressed in *Escherichia coli* as fusions with glutathione S-transferase. *Gene* 67, 31–40.
- Subota I, Julkowska D, Vincensini L, Reeg N, Buisson J, Blisnick T, Huet D, Perrot S, SANTI-Rocca J, Duchateau M, et al. (2014). Proteomic analysis of intact flagella of procyclic *Trypanosoma brucei* cells identifies novel flagellar proteins with unique sub-localisation and dynamics. *Mol Cell Proteomics* 13, 1769–1786.
- Subota I, Rotureau B, Blisnick T, Ngwabyt S, Durand-Dubief M, Engstler M, Bastin P (2011). ALBA proteins are stage regulated during trypanosome development in the tsetse fly and participate in differentiation. *Mol Biol Cell* 22, 4205–4219.
- Vale RD (2003). The molecular motor toolbox for intracellular transport. *Cell* 112, 467–480.
- Walczak-Sztulpa J, Eggenschwiler J, Osborn D, Brown DA, Emma F, Klingenberg C, Hennekam RC, Torre G, Garshabi M, Tzschach A, et al. (2010). Cranioectodermal dysplasia, Sensenbrenner syndrome, is a ciliopathy caused by mutations in the IFT122 gene. *Am J Hum Gen* 86, 949–956.
- Wang Z, Fan ZC, Williamson SM, Qin H (2009). Intraflagellar transport (IFT) protein IFT25 is a phosphoprotein component of IFT complex B and physically interacts with IFT27 in *Chlamydomonas*. *PLoS One* 4, e5384.
- Wang Z, Morris JC, Drew ME, Englund PT (2000). Inhibition of *Trypanosoma brucei* gene expression by RNA interference using an integratable vector with opposing T7 promoters. *J Biol Chem* 275, 40174–40179.
- Williams CL, Li C, Kida K, Inglis PN, Mohan S, Semenc L, Bialas NJ, Stupay RM, Chen N, Blacque OE, et al. (2011). MKS and NPHP modules cooperate to establish basal body/transition zone membrane associations and ciliary gate function during ciliogenesis. *J Cell Biol* 192, 1023–1041.
- Wirtz E, Leal S, Ochatt C, Cross GA (1999). A tightly regulated inducible expression system for conditional gene knock-outs and dominant-negative genetics in *Trypanosoma brucei*. *Mol Biochem Parasitol* 99, 89–101.
- Wren KN, Craft JM, Tritschler D, Schauer A, Patel DK, Smith EF, Porter ME, Kner P, Lehtreck KF (2013). A differential cargo-loading model of ciliary length regulation by IFT. *Curr Biol* 23, 2463–2471.